

Shedding New Light on Kaon-Nucleon/Nuclei Interaction and Its Astrophysical Implications with the AMADEUS Experiment at DAΦNE

A. Scordo^{1,a)}, M. Bazzi¹, G. Bellotti², C. Berucci³, D. Bosnar⁴, A.M. Bragadireanu⁵, A. Clozza¹, M. Cargnelli³, C. Curceanu¹, A. Dawood Butt², R. Del Grande¹, L. Fabbietti⁶, C. Fiorini², F. Ghio¹, C. Guaraldo¹, M. Iliescu¹, P. Levi Sandri¹, J. Marton³, D. Pietreanu⁵, K. Piscicchia^{1,7}, H. Shi¹, D. Sirghi^{1,5}, F. Sirghi^{1,5}, I. Tucakovic⁸, O. Vazquez Doce⁴, W. Wiedmann³ and J. Zmeskal³

¹*INFN Laboratori Nazionali di Frascati, Frascati (Roma), Italy.*

²*Politecnico di Milano, Dipartimento di Elettronica, Informazione e Bioingegneria and INFN Sezione di Milano, Milano, Italy.*

³*Stefan-Meyer-Institut für subatomare Physik, Vienna, Austria.*

⁴*Physics Department, University of Zagreb, Zagreb, Croatia.*

⁵*Horia Hulubei National Institute of Physics and Nuclear Engineering (IFIN-HH), Magurele, Romania.*

⁶*Excellence Cluster Universe, Technische Universität München, Garching, Germany.*

⁷*Museo Storico della Fisica e Centro Studi e Ricerche "Enrico Fermi", Roma, Italy.*

⁸*Ruder Bošković Institute, Bijenička cesta 54, Zagreb, Croatia.*

^{a)}Corresponding author: alessandro.scordo@lnf.infn.it

Abstract. The AMADEUS experiment deals with the investigation of the low-energy kaon-nuclei hadronic interaction at the DAΦNE collider at LNF-INFN, which is fundamental to respond longstanding questions in the non-perturbative QCD strangeness sector. The antikaon-nucleon potential is investigated searching for signals from possible bound kaonic clusters, which would open the possibility for the formation of cold dense baryonic matter. The confirmation of this scenario may imply a fundamental role of strangeness in astrophysics. AMADEUS step 0 consisted in the reanalysis of 2004/2005 KLOE dataset, exploiting K^- absorptions in H, ^4He , ^9Be and ^{12}C in the setup materials. In this paper, together with a review on the multi-nucleon K^- absorption and the particle identification procedure, the first results on the $\Sigma^0\text{p}$ channel will be presented including a statistical analysis on the possible accommodation of a deeply bound state.

INTRODUCTION

The AMADEUS experiment [1, 2] deals with the study of the low-energy interactions of the negatively charged kaons with light nuclei. Such type of physics, extremely important for the understanding of the non-perturbative QCD in the strangeness sector, has important consequences, going from hadron and nuclear physics to astrophysics. In this context, useful information can be obtained from the strength of the K^- binding in nuclei. The investigation of the absorptions of K^- inside the KLOE Drift Chamber (DC) was originally motivated by the prediction of the formation of deeply bound kaonic nuclear states [3, 4]. Their binding energies and widths could be determined by studying their decays into hyperons and nucleons. Also intimately connected with the kaon-nucleon potential is the $\Lambda(1405)$ resonance, of which the still puzzling nature can be investigated within AMADEUS [5]. The study of the KN interaction at low energies is of interest not only for quantifying the meson-baryon potential with strange content, but also because of its impact on models describing the structure of neutron stars (NS) [6]. The KN potential is attractive, as theory predicts [7] and kaonic atoms confirm [8], and this fact leads to the formulation of hypotheses about antikaon role inside the dense interior of neutron stars; one or more nucleons could be kept together by the strong attractive

interaction between antikaons and nucleons and the so-called kaonic bound states, as ppK^- or $ppnK^-$, might be formed. The observation of such states and the measurements of their binding energies and widths, would provide a quantitative measurement of the KN interaction in vacuum, representing an important reference for the investigation of the in-medium properties of kaons. From the experimental point of view, two main approaches have been used for studying the K^-pp cluster: $p-p$ and heavy ion collisions [9] [10], and in-flight or stopped K^- interactions in light nuclei. For the second, results have been published by the FINUDA [11] and KEK-PS E549 collaborations [12]. The interpretation of both results is far from being conclusive, and it requires an accurate description of the single and multi-nucleon absorption processes that a K^- would undergo when interacting with light nuclei. From the analysis of the KLOE 2004-2005, information on both the strength of the K^- binding in nuclei and the in-medium modification of the Σ^* and Λ^* resonances properties can be extracted by analysing, respectively, the $\Lambda/\Sigma - p, d, t$ channels and at the resonances decay channels $\Lambda/\Sigma - \pi$. In this paper we focus, in particular, on the analysis of the $\Sigma^0 p$ final state produced in absorption processes of K^- on two or more nucleons, occurring in the KLOE DC entrance wall, and on the search for a signature of the $ppK^- \rightarrow \Sigma^0 + p$ kaonic bound state. A more detailed description of the analysis procedures can be found in [13].

The DAΦNE collider and the KLOE detector

DAΦNE [14] (Double Anular Φ-factory for Nice Experiments) is a double ring e^+e^- collider, designed to work at the center of mass energy of the ϕ particle $m_\phi = (1019.456 \pm 0.020) MeV/c^2$. The ϕ meson decay produces charged kaons (with $BR(K^+K^-) = 48.9 \pm 0.5\%$) with low momentum ($\sim 127 MeV/c$) which is ideal either to stop them, or to explore the products of the low-energy nuclear absorptions of K^- s. The KLOE detector [15] is centered around the interaction region of DAΦNE and is characterised by a $\sim 4\pi$ geometry and an acceptance of $\sim 98\%$; it consists of a large cylindrical Drift Chamber (DC) and a fine sampling lead-scintillating fibers calorimeter, all immersed in an axial magnetic field of 0.52 T, provided by a superconducting solenoid. The DC [16] has an inner radius of 0.25 m, an outer radius of 2 m and a length of 3.3 m. The DC entrance wall composition is 750 μm of carbon fibre and 150 μm of aluminium foil. Dedicated GEANT MonteCarlo simulations of the KLOE apparatus were performed to estimate the percentages of K^- absorptions in the materials of the DC entrance wall (the K^- absorption physics were treated by the GEISHA package). Out of the total number of kaons interacting in the DC entrance wall, about 81% results to be absorbed in the carbon fibre component and the residual 19% in the aluminium foil. The KLOE DC is filled with a mixture of helium and isobutane (90% in volume 4He and 10% in volume C_4H_{10}). The chamber is characterised by excellent position and momentum resolutions. Tracks are reconstructed with a resolution in the transverse $R - \phi$ plane of $\sigma_{R\phi} \sim 200 \mu m$ and a resolution along the z-axis of $\sigma_z \sim 2 mm$. The transverse momentum resolution for low momentum tracks ($(50 < p < 300) MeV/c$) is $\frac{\sigma_{pT}}{pT} \sim 0.4\%$. The KLOE calorimeter [17] is composed of a cylindrical barrel and two endcaps, providing a solid angle coverage of 98%. The volume ratio (lead/fibres/glue=42:48:10) is optimised for a high light yield and a high efficiency for photons in the range (20-300) MeV/c . The position of the cluster along the fibres can be obtained with a resolution $\sigma_{\parallel} \sim 1.4 cm / \sqrt{E(GeV)}$. The resolution in the orthogonal direction is $\sigma_{\perp} \sim 1.3 cm$. The energy and time resolutions for photon clusters are given by $\frac{\sigma_E}{E_\gamma} = \frac{0.057}{\sqrt{E_\gamma(GeV)}}$ and $\sigma_t = \frac{57 ps}{\sqrt{E_\gamma(GeV)}} \oplus 100 ps$. As a step 0 of AMADEUS, we analysed the 2004-2005 KLOE collected data, for which the dE/dx information of the reconstructed tracks is available (dE/dx represents the truncated mean of the ADC collected counts due to the ionisation in the DC gas). An important contribution of in-flight K^- nuclear captures, in different nuclear targets from the KLOE materials, was evidenced and characterised, enabling to perform invariant mass spectroscopy of in-flight K^- nuclear captures [18].

Preliminary results of the data analyses

The investigation of the negatively charged kaons interactions in nuclear matter is performed through the reconstruction of hyperon-pion and hyperon-nucleon/nucleus correlated pairs productions, following the K^- absorptions in H, 4He , 9Be and ^{12}C . The investigation of the K^- multi-nucleon absorptions and the properties of possible antikaon multi-nucleon bound states proceeds through the analyses of the $\Lambda/\Sigma - p, d, t$, correlations; this last channel is, in particular, extremely promising for the search and characterisation in different nuclear targets of the extremely rare four nucleon absorption process. The search for the $\Lambda(1405)$ is performed through its decay into $\Sigma^0\pi^0$ (purely isospin I=0) and $\Sigma^+\pi^-$ (also the analysis of the $\Sigma^-\pi^+$ decay channel started recently with a characterisation of neutron clusters

in the KLOE calorimeter). The line shapes of the three combinations $(\Sigma\pi)^0$ were recently obtained, for the first time, in a photoproduction experiment [19]; as the line-shapes of the three invariant mass spectra were found to be different, a comparative study with K^-N production is of extreme interest. Moreover, a precise measurement of the $\frac{\Sigma^+\pi^-}{\Sigma^-\pi^+}$ production ratio in different targets can unveil the nature of the Λ^* state, by observing modifications of its parameters as a function of the density [20, 21]. To conclude, given the excellent resolution for the $\Lambda\pi^-$ invariant mass, the analysis of the $\Lambda\pi^-$ (isospin $I=1$) production, both from direct formation process and from internal conversion of a primary produced Σ hyperon ($\Sigma N \rightarrow \Lambda N'$) is presently ongoing. Our aim is to measure, for the first time, the module of the non-resonant transition amplitude (compared with the resonant Σ^{*-}) below threshold.

The $\Lambda(1116)$ selection

The presence of a hyperon always represents the signature of a K^- hadronic interaction inside the KLOE setup materials. Most of the analyses introduced in the previous section then start with the identification of a $\Lambda(1116)$, through the reconstruction of the $\Lambda \rightarrow p + \pi^-$ ($\text{BR} = 63.9 \pm 0.5\%$) decay vertex. In figure 1 left the dE/dx versus momentum scatterplot for the finally selected protons is shown, where the function used for the selection of protons is displayed in red. The typical signature of pions in dE/dx versus momentum can be also seen in figure 1 left illustrating the efficient rejection of π^+ contamination in a broad range of momentum. A minimum track length of 30 cm is required, and a common vertex is searched for all the $p - \pi^-$ pairs in each event. When found, the common vertex position is added as an additional constraint for the track refitting. The module of the momentum and the vector cosines are redefined for both tracks, taking into account for the energy loss in the gas and the various crossed materials (signal and field wires, DC wall, beam pipe) when tracks are extrapolated back through the detector. As a final step for the identification of Λ decays, the vertices are cross checked with quality cuts using the minimum distance between tracks (minimum distance < 3.2 cm) and the chi-square of the vertex fit. A spatial resolution below 1 mm is achieved for vertices found inside the DC volume (evaluated with Monte Carlo). The invariant mass $m_{p\pi^-}$, calculated under the p and π^- mass hypothesis, is shown in figure 1 right. The Gaussian fit gives a mass of $1115.723 \pm 0.003 \text{ MeV}/c^2$ and an excellent resolution (σ) of $0.3 \text{ MeV}/c^2$, confirming the unique performances of KLOE for charged particles (the systematics, depending on the momentum calibration of the KLOE setup, are presently under evaluation).

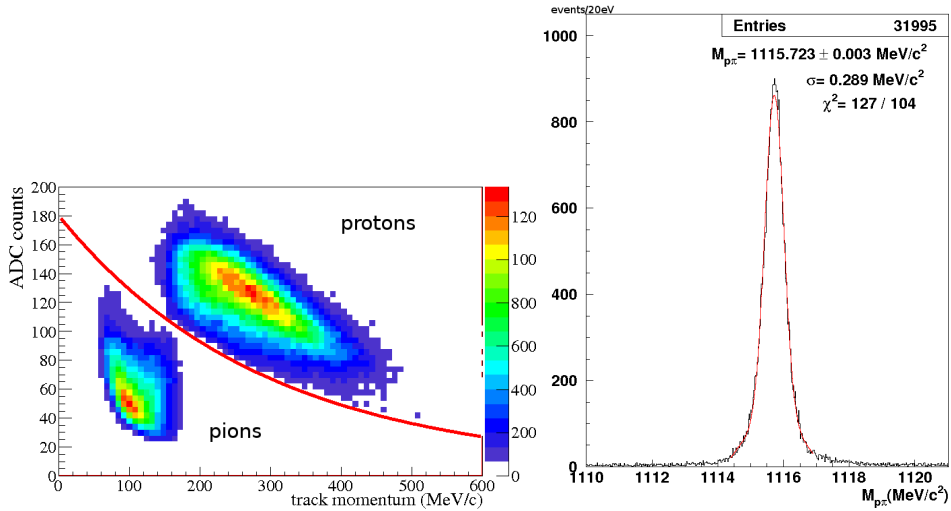


FIGURE 1. Left: dE/dx (in ADC counts) vs. momentum for the selected proton (up) and pion (down) tracks in the final selection. The proton selection functions is displayed in red. Right: $m_{p\pi^-}$ invariant mass spectrum for the selected pion-proton pairs.

This is the common procedure for all the analysed channels starting with the initial search of a Λ as a signature for the hadronic interaction of the K^- . Cuts on the radial position (ρ_Λ) of the Λ decay vertex were optimised in order to separate the two samples of K^- absorption events occurring in the DC wall and the DC gas: $\rho_\Lambda = 25 \pm 1.2$ cm and $\rho_\Lambda > 33$ cm, respectively. The ρ_Λ limits were set based on MC simulations and a study of the Λ decay path. In

particular, the $\rho_\Lambda = 25 \pm 1.2$ cm cut guarantees, for the first sample, a contamination of K^- interactions in gas as low as $(5.5^{+1.3}_{-1.8}\%)$.

$\Sigma^0 p$ analysis

After the Λ search, a common vertex between the Λ candidate and an additional proton track is searched for. The obtained resolution on the radial coordinate for the Λp vertex is 12 mm, while its invariant mass resolution is found to be, from MC studies, equal to $1.1 \text{ MeV}/c^2$. The Σ^0 candidates are identified through their decay into $\Lambda\gamma$ pairs. After the reconstruction of a Λp pair, the photon selection is carried out via its identification in the EMC. Photon candidates are selected by applying a cut on the difference between the EMC time measurement and the expected time of arrival of the photon within $-1.2 < \Delta t < 1.8 \text{ ns}$. Then, the $\Sigma^0 p$ invariant mass, opening angle, and the individual Σ^0 and proton momenta distributions are considered simultaneously in a global fit to extract the contributions of the various absorption processes. The processes that are taken into account in the fit of the experimental data are:

- $K^- A \rightarrow \Sigma^0 - (\pi) p_{spec}(A')$
- $K^- pp \rightarrow \Sigma^0 - p(2NA)$
- $K^- ppn \rightarrow \Sigma^0 - p - n(3NA)$
- $K^- ppnn \rightarrow \Sigma^0 - p - n - n(4NA)$

where A is the atomic number of the target nucleus, p_{spec} is the spectator proton, A' is the atomic number of the residual nucleus and 2/3/4NA stands for 2/3/4-nucleons absorption. This list includes the K^- absorption on two nucleons with and without final state interaction (FSI) for the $\Sigma^0 p$ state and processes involving more than two nucleons in the initial state. These contributions are either extracted from experimental data samples or modelled via simulations. Two kinds of background contribute to the analysed $\Sigma^0 p$ final state: the machine background and the events with $\Lambda\pi^0 p$ in the final state. Both are quantified using experimental data [13]. The obtained fit is shown in figure 2 and the results are summarised in table 1.

TABLE 1. Production probability of the $\Sigma^0 p$ final state for different intermediate processes normalised to the number of stopped K^- in the DC wall. The statistical and systematic errors are shown as well [13].

Process	yield / $K^-_{stop} \times 10^{-2}$	$\sigma_{stat} \times 10^{-2}$	$\sigma_{syst} \times 10^{-2}$
2NA-QF	0.127	± 0.019	$+0.004$ -0.008
2NA-FSI	0.272	± 0.028	$+0.022$ -0.023
Tot 2NA	0.376	± 0.033	$+0.023$ -0.032
3NA	0.274	± 0.069	$+0.044$ -0.021
Tot 3 body	0.546	± 0.074	$+0.048$ -0.033
4NA + bkg.	0.773	± 0.053	$+0.025$ -0.076

The final fit results deliver the contributions of the different channels to the analysed $\Sigma^0 p$ final state. The best fit delivers a χ^2 of 0.85. The emission rates extracted from the fit are normalised to the total number of stopped antikaons. The fit results lead to the first measurements of the genuine 2NA-QF for the final state $\Sigma^0 p$ in reactions of stopped K^- on targets of ^{12}C and ^{27}Al . This contribution is found to be only 12% of the total absorption cross-section. The last step of the analysis consists in the search of the ppK^- bound state produced in K^- interaction with nuclear targets, decaying into a $\Sigma^0 p$ pair. The ppK^- are simulated similarly to the 2NA-QF process but sampling the mass of the ppK^- state with a Breit-Wigner distribution, rather than the Fermi momenta of the two nucleons in the initial state. The event kinematic is obtained by imposing the momentum conservation of the ppK^- residual nucleus system. Different values for the binding energy and width varying within $15 - 75 \text{ MeV}/c^2$ and $30 - 70 \text{ MeV}/c^2$ in steps of 15 and 20 MeV/c^2 , respectively, are tested. This range has been selected according to several theoretical predictions present in literature and taking into account the experimental resolution. The global fit is repeated adding the ppK^- . The best fit ($\chi^2/ndf = 0.807$) is obtained for a ppK^- candidate with a binding energy of $45 \text{ MeV}/c^2$ and a width of $30 \text{ MeV}/c^2$, respectively. Figure 3 shows the results of the best fit for the $\Sigma^0 p$ invariant mass and proton momentum distributions where the ppK^- bound state contribution is shown in green.

The resulting yield normalised to the number of stopped K^- is $ppK^-/K^-_{stop} = (0.044 \pm 0.009_{stat}^{+0.004}_{-0.005} syst) \times 10^{-2}$.

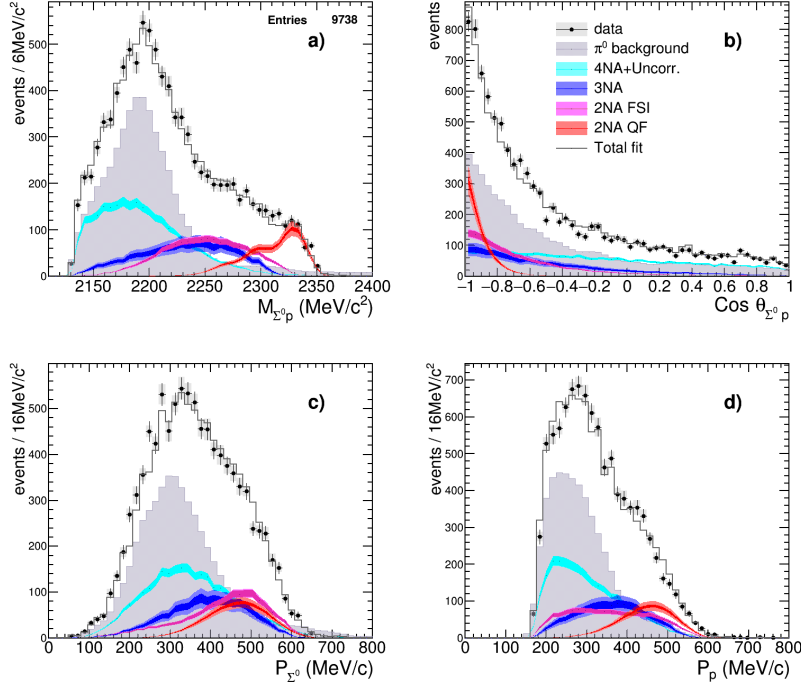


FIGURE 2. Experimental distributions of the $\Sigma^0 p$ invariant mass, $\cos(\theta_{\Sigma^0 p})$, Σ^0 and proton momentum together with the results of the global fit. The experimental data after the subtraction of the machine background are shown by the black circles, the systematic errors are represented by the boxes and the coloured histograms correspond to the fitted signal distributions where the light-coloured bands show the fit errors and the darker bands represent the symmetrised systematic errors. The gray line show the total fit distributions (see [13] for details).

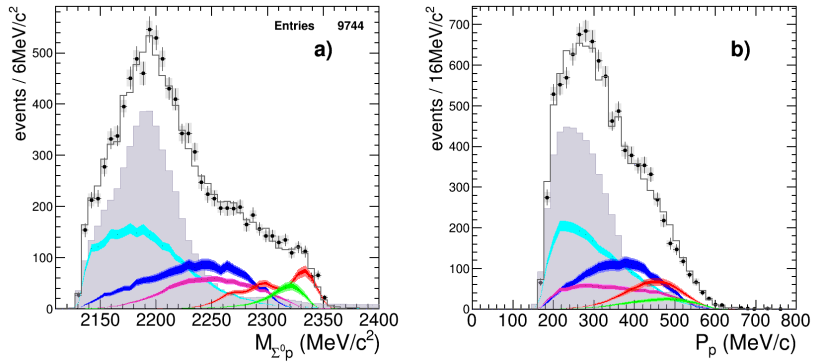


FIGURE 3. $\Sigma^0 p$ invariant mass and proton momentum distributions together with the results of the global fit including the ppK^- . The different contributions are labeled as in figure 2 and the green histograms represent the ppK^- signal

The F-test conducted to compare the simulation models with and without the ppK^- signal gave a significance of the result of only 1σ for the ppK^- yield result [13]. This shows that although the measured spectra are compatible with the hypothesis of a contribution of a deeply bound state, the significance of the result is not sufficient to claim the discovery of this state.

Conclusions and perspectives

The broad experimental program of AMADEUS, dealing with the non-perturbative QCD in the strangeness sector, is supported by the quest for high precision and statistics measurements, able to set more stringent constraints on the existing theoretical models. We demonstrated the capabilities of the KLOE detector to perform high quality physics (taking advantage of the unique features of the DAΦNE factory) in the open sector of strangeness nuclear physics. Our investigations, presently spread on a wide spectrum of physical processes, represent the most ambitious and systematic effort in this field. In particular, in this report we have presented the analysis of the K^- absorption processes leading to the $\Sigma^0 p$ state measured with the KLOE detector. It was shown that the full kinematics of this final state can be reconstructed and a global fit of the kinematic variables allows to pin down quantitatively the various contributing processes. Also, the possibility to accommodate a signal from a ppK^- bound state has been investigated. We proved the possibility to deliver very accurate and valuable results in the strangeness sector, in particular for what concerns the comprehension of the KN potential, by studying all the possible channels following a K^- absorption on one or several nucleons, for very low momentum kaons. For the future, a dedicated AMADEUS setup, with dedicated gaseous and solid targets, where to enhance the fraction of stopped kaons, is under study.

ACKNOWLEDGMENTS

We thank all the KLOE Collaboration and the DAΦNE staff for the fruitful collaboration.

We acknowledge the Croatian Science Foundation under Project No. 1680.

Part of this work was supported by the European Community-Research Infrastructure Integrating Activity “Study of Strongly Interacting Matter” (HadronPhysics2, Grant Agreement No. 227431, and HadronPhysics3 (HP3) Contract No. 283286) under the EU Seventh Framework Programme.

REFERENCES

- [1] AMADEUS Letter of Intent, http://www.lnf.infn.it/esperimenti/siddharta/LOI_AMDEUS_March2006.pdf
- [2] The AMADEUS collaboration, LNF preprint, LNF/9607/24(IR) (2007)
- [3] S. Wycech, Nucl. Phys. A 450, 399c (1986).
- [4] Y. Akaishi and T. Yamazaki, Phys. Rev. C 65, 044005 (2002).
- [5] T. Hyodo, D. Jido, Prog. Part. Nucl. Phys. 67 (2012) 55.
- [6] A. E. Nelson and D. B. Kaplan, Phys. Lett. B 192, 193 (1987).
- [7] C. Fuchs, Prog. Part. Nucl. Phys. 56, 1 (2006), nuclth/0507017.
- [8] M. Bazzi et al. (SIDDHARTA Coll.), Phys. Lett. B 704, 113 (2011).
- [9] K. Suzuki et al., Nucl. Phys. A 827, 312C-314C (2012).
- [10] G. Agakishiev et al., Phys. Lett. C 85, 035203 (2012).
- [11] M. Agnello et al., Phys. Rev. Lett. 94, 919303 (2005).
- [12] T. Suzuki et al., Mod. Phys. Lett. A 23, 2520-2523 (2008).
- [13] O. Vazquez Doce et al, arxiv:151.04496v1 [nucl-ex].
- [14] R. Baldini et al., Proposal for a Phi-Factory, report LNF-90/031(R) (1990).
- [15] F. Bossi et al. (KLOE coll.), Nuovo Cim. 31 531-623 (2008).
- [16] M. Adinolfi et al., [KLOE Collaboration], Nucl. Inst. Meth. A 488, (2002) 51.
- [17] M. Adinolfi et al. [KLOE Collaboration], Nucl. Inst. Meth. A 482, (2002) 368.
- [18] K. Piscicchia et al. e-Print: arXiv:1304.7165
- [19] K. Moriya et al. (CLAS Collaboration) Phys. Rev. C 87, 035206 (2013)
- [20] L. R. Staronski, S. Wycech, Nucl. Phys. 13 (1987) 1361
- [21] A. Ohnishi et al., Phys. Rev. C 56 5 (1997) 2767